Accessing the dark exciton spin in deterministic quantum-dot microlenses

Tobias Heindel, Alexander Thoma, Ido Schwartz, Emma R. Schmidgall, Liron Gantz, Dan Cogan, Max Strauß, Peter Schnauber, Manuel Gschrey, Jan-Hindrik Schulze, Andre Strittmatter, Sven Rodt, David Gershoni, and Stephan Reitzenstein

Citation: APL Photonics **2**, 121303 (2017);
View online: https://doi.org/10.1063/1.5004147
View Table of Contents: http://aip.scitation.org/toc/app/2/12
Published by the American Institute of Physics

Accessing the dark exciton spin in deterministic quantum-dot microlenses

Tobias Heindel,[1,a] Alexander Thoma,[1] Ido Schwartz,[2] Emma R. Schmidgall,[2,b] Liron Gantz,[2] Dan Cogan,[2] Max Strauß,[1] Peter Schnauber,[1] Manuel Gschrey,[1] Jan-Hindrik Schulze,[1] Andre Strittmatter,[1,c] Sven Rodt,[1] David Gershoni,[2] and Stephan Reitzenstein[1]

[1]*Institut für Festkörperphysik, Technische Universität Berlin, 10623 Berlin, Germany*
[2]*The Physics Department and the Solid State Institute, Technion-Israel Institute of Technology, 32000 Haifa, Israel*

(Received 11 September 2017; accepted 28 November 2017; published online 19 December 2017)

The dark exciton state in semiconductor quantum dots (QDs) constitutes a long-lived solid-state qubit which has the potential to play an important role in implementations of solid-state-based quantum information architectures. In this work, we exploit deterministically fabricated QD microlenses which promise enhanced photon extraction, to optically prepare and read out the dark exciton spin and observe its coherent precession. The optical access to the dark exciton is provided via spin-blockaded metastable biexciton states acting as heralding states, which are identified by deploying polarization-sensitive spectroscopy as well as time-resolved photon cross-correlation experiments. Our experiments reveal a spin-precession period of the dark exciton of (0.82 ± 0.01) ns corresponding to a fine-structure splitting of (5.0 ± 0.7) μeV between its eigenstates $|\uparrow\Uparrow \pm \downarrow\Downarrow\rangle$. By exploiting microlenses deterministically fabricated above pre-selected QDs, our work demonstrates the possibility to scale up implementations of quantum information processing schemes using the QD-confined dark exciton spin qubit, such as the generation of photonic cluster states or the realization of a solid-state-based quantum memory. https://doi.org/10.1063/1.5004147

The quest for so-called quantum bits (qubits) satisfying the stringent demands of future quantum computation and quantum communication scenarios is actively pursued world-wide.[1] In this context, solid-state-based matter qubits are of particular interest due to their capability for device integration,[2] which nowadays enables the development of sophisticated quantum-light sources.[3–6] In recent years, the coherent properties of bright excitons (BEs)[7,8] as well as single electron-[9] and hole-[10] spins confined in semiconductor quantum dots[11] (QDs) have been explored extensively. The BE is particularly useful as a qubit since its coherent state can be initialized, controlled,[12] and read out[13] using single picosecond-long optical pulses.[14] The use of the BE for quantum information processing tasks, however, is still limited due to its relatively short radiative lifetime (≈1 ns). The QD-confined dark exciton (DE), on the other hand, has been demonstrated to constitute an extremely long-lived (≈1 μs)[15] matter qubit, which interestingly can also be optically accessed, using either all-optical[16] or magneto-optical[17,18] schemes. Similar to the BE, the DE can be initialized[19] and read out using a short optical pulse, while it features long coherence times (≈100 ns).[20] Exploiting these features, the DE was recently used as an entangler for the on-demand generation of entangled multi-photon cluster states.[21] The optical access to the DE is enabled via excited biexcitonic states containing two charge carriers with parallel spins.[22,23] Such states are usually spin-blockaded from relaxation to the

[a]Electronic mail: tobias.heindel@tu-berlin.de
[b]Present address: Department of Physics, University of Washington, Seattle, WA 98195, USA.
[c]Present address: Abteilung für Halbleiterepitaxie, Otto-von-Guericke Universität, 39106 Magdeburg, Germany.

biexciton ground state in which the two electrons and two holes have anti-parallel spins. To date, only one group succeeded in optically accessing the DE spin via biexcitonic spin-triplet states.[16] This first demonstration used a simple planar and non-deterministic sample, offering only limited photon extraction. To push experiments beyond the proof-of-principle stage, however, requires larger photon harvesting efficiencies only achievable with advanced photonic microstructures. Additionally, the sample material used in Ref. 16 and subsequent work (see Ref. 24 for a recent review) was grown by molecular beam epitaxy (MBE) exclusively. A proof that the scheme of optically accessing the DE spin is possible also in devices grown by other techniques is still pending. Thus scalable implementations of the scheme presented in Ref. 16 remained elusive so far.

In this work, we employ deterministically fabricated microlenses above pre-selected QDs grown by metal-organic chemical vapor deposition (MOCVD) to optically prepare and read out the DE spin qubit and observe its coherent precession. The use of a geometric microlens approach, rather than a narrow-band microcavity, is highly beneficial in our experiment, as the lens provides efficient photon extraction over a wide spectral range. This allows for a simultaneous access to multiple, energetically separated QD states. Our experiments performed with deterministic photonic devices clearly reveal the coherent precession of the DE's spin, which provides promises for scalable implementations of quantum information processing using the QD-confined DE as the solid-state-based spin qubit.

The samples utilized for our experiments were grown by MOCVD on a GaAs (001)-substrate. A layer of self-organized InGaAs QDs capped with 400 nm of GaAs is located above a distributed Bragg reflector with 23 AlGaAs/GaAs mirror-pairs. The capping layer provides the material for the fabrication of microlenses via 3D *in situ* electron-beam lithography,[25,26] where preselected target QDs are deterministically integrated within monolithic microlenses [see Fig. 1(a), inset]. For details on the

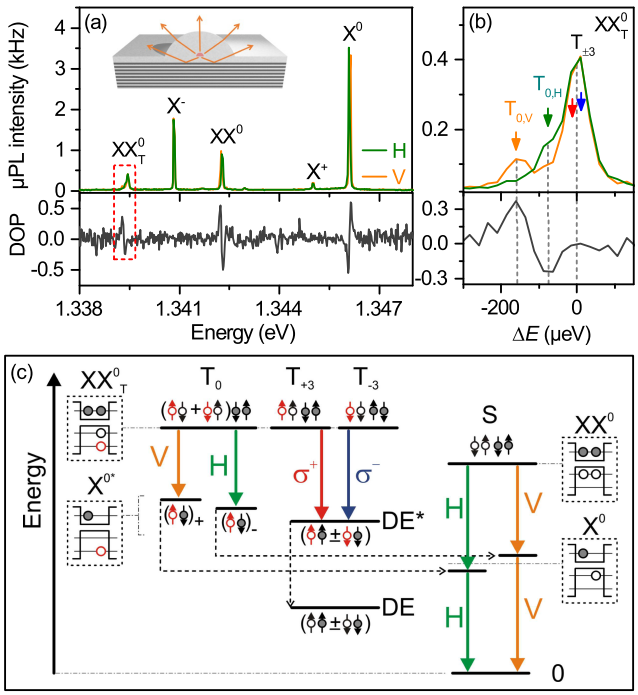

FIG. 1. (a) Polarization sensitive micro-photoluminescence (μPL) spectra (upper panel) and extracted rectilinear (HV) degree of polarization (DOP) (lower panel) of a single QD microlens. The relevant excitonic states are labeled: bright exciton (X^0), biexciton (XX^0), charged trions (X^- and X^+), and emission of the spin-blockaded biexciton triplet (XX^0_T). Inset: Schematic of a deterministic microlens used for our experiments. A single QD is integrated within a monolithic microlens above a lower Bragg mirror. (b) PL from the spin-blockaded biexciton triplet states (XX^0_T) on an expanded energy scale, revealing two cross rectilinearly polarized components resulting from the XX^0_{T0} biexciton and twofold degenerate unpolarized $XX^0_{T\pm3}$ biexcitons. (c) Schematic description of the biexciton and exciton energy levels and optical transitions illustrating the selection rules observed in (a) and (b). Empty (filled) circles indicate holes (electrons), and solid (dashed) arrows represent radiative (non-radiative) relaxation processes. Red (black) empty circles indicate holes located in the QD's p-shell (s-shell).

sample layout, microlens fabrication, and quantum optical properties, we refer to the recent review in Ref. 27. Microlenses based on the layout used in this work typically show photon extraction efficiencies of 20-30% at a numerical aperture (NA) of 0.4.[25,28] Noteworthy, similar coherence times were observed for photons emitted by the BE states of MOCVD-grown QDs embedded in microlenses[29,30] and MBE-grown QDs in planar cavities.[32] This indicates that the microlens fabrication does not lead to a noticeable degradation of the optical properties of the QDs. Optical experiments were performed in a confocal micro-photoluminescence (μPL) setup with the sample mounted onto the cold finger of a cryostat at temperatures in the range of 4–20 K. The sample is excited using a wavelength-tunable continuous-wave (CW) titanium-sapphire laser at a wavelength between 850 and 880 nm, corresponding to the wetting-layer excitation for the present QDs. The PL from the QD microlenses is collected via a microscope objective (NA: 0.40 or 0.85) and spectrally analyzed using grating spectrometers (spectral resolution: 25 μeV). Correlations between photons emitted from different spectral lines are studied by means of polarization sensitive intensity cross-correlation measurements.[31,32] Photons are detected at the output of the monochromators via fiber-coupled silicon-based single-photon counting modules (SPCMs) or nanowire-based superconducting single-photon detectors (SSPDs) with a timing resolution of 250 ps and 90 ps, respectively. Time-resolved coincidence measurements are enabled using time-correlated single-photon counting electronics.

Figure 1(a) shows the μPL spectra of a deterministic QD microlens recorded in rectilinear (HV) polarization bases at a temperature of T = 7 K. Various spectral lines are observed and identified using their typical polarization and excitation intensity dependencies. Emission of the bright exciton (X^0), the ground-state biexciton (XX^0) as well as the negatively and positively charged trions (X^-, X^+) are identified. The polarization selection rules of these spectral lines can be inferred from the lower panel of Fig. 1(a), where the degree of polarization (DOP) in rectilinear basis is presented according to DOP = $(I_H - I_V)/(I_H + I_V)$, where I_H and I_V refer to the μPL intensity in horizontal (H) and vertical (V) polarization, respectively. Both, the X^0 and XX^0 lines are composed of two cross-linearly polarized components, exhibiting a fine-structure splitting of $\Delta E_{FSS,BE} = (36 \pm 1)$ μeV. The trion lines X^- and X^+, on the other hand, are unpolarized, as expected. At the low energy tail of the spectrum, additional spectral lines are visible at 1.3395 eV. These lines are more clearly seen in the expanded energy scale of Fig. 1(b), which reveals a spectral triplet composed of one unpolarized line and two, about a factor of 4 weaker, cross-rectilinearly polarized lines. As explained in the following, these emission lines can be attributed to emission from the biexcitonic spin-triplet states XX^0_T (subscript indicating the respective spin configuration). In contrast to the common spin-singlet biexciton state XX^0, the biexcitonic triplet states are comprised of two s-shell electrons and two holes, one in the s-shell and one in the p-shell. The possible spin-configurations of the triplet and singlet states are illustrated in the energy level scheme in Fig. 1(c). In case of antiparallel hole spins, the total spin vanishes and the respective state XX^0_{T0} radiatively decays via recombination of a s-shell electron-hole pair under the emission of one H- or V-polarized photon. Subsequently, the QD is left in either the symmetric or antisymmetric superposition of the excited exciton states $X^{0*}_{\pm}$, which reveal a fine structure splitting similar to the bright exciton states X^0. The $X^{0*}_{\pm}$ states quickly relax non-radiatively to the X^0 states, which in turn decay radiatively by emitting one V- or H-polarized photon. Therefore, the biexcitonic triplet state XX^0_{T0}, the bright exciton state X^0, and the ground state (empty QD) constitute a radiative cascade, similar to the XX^0-X^0 cascade. Importantly, the two photons emitted by the XX^0_{T0}-X^0 cascade are cross-rectilinearly correlated with respect to their polarization due to the underlying selection rules.[22] This behavior is opposite to the common XX^0-X^0 cascade, which is co-rectilinearly correlated. This picture changes if the initial spin-triplet state is constituted of two holes with parallel spin-projection. The two resulting states $XX^0_{T\pm3}$ are almost degenerate in energy and have a total spin projection of ±3 on the QD growth axis. In this case, the radiative recombination of the s-shell electron-hole pair results in the emission of a left- (L) or right- (R) hand circularly polarized photon, leaving the QD in an excited dark exciton state (DE*) with parallel spin-configuration. After a fast spin-preserving non-radiative relaxation of the hole from the p- to the s-shell, the QD ends in the DE ground state X^0_{DE}. Therefore, the detection of a photon stemming from the $XX^0_{T\pm3}$-DE* transition heralds the formation of the DE state.[16]

To verify the selection rules and correlations described earlier, we performed polarization-sensitive time-resolved photon correlation measurements on both biexciton cascades using the SPCMs. The excitation power is hereby set to a point where the PL from the XX^0 line is approximately half of that from the X^0 line ($P = 9\ \mu$W). Figure 2(a) shows the normalized cross-correlation events of the biexciton-exciton XX^0-X^0 emission as a function of the time between detection events, where the biexciton photon detection is chosen to trigger the coincidence counting. The radiative cascade reveals itself in a pronounced bunching in the co-rectilinearly polarized coincidences (VV), while the cross-rectilinearly polarized coincidences (VH) are strongly suppressed. This results in a positive degree of polarization correlation $C_{\mathrm{HV}}(\tau) = (g^{(2)}_{\mathrm{VV}} - g^{(2)}_{\mathrm{VH}})/(g^{(2)}_{\mathrm{VV}} + g^{(2)}_{\mathrm{VH}})$ during the radiative cascade [cf. Fig. 2(b)], where the non-ideal visibility is due to the relatively strong excitation and the finite temporal resolution of the used SPCMs. Similar behavior is observed in Fig. 2(c), where photon coincidences resulting from the indirect radiative cascade of XX^0_{T0} and X^0 are presented. Again a pronounced bunching signifies the biexcitonic origin of the initial state XX^0_{T0}. The polarization selection rules, however, are reversed in this case. As a result, a negative degree of polarization correlation ($C_{\mathrm{HV}} < 0$) is obtained in Fig. 2(d). This behavior confirms the selection rules illustrated in Fig. 1(c) in agreement with the observations reported in Ref. 22, which allows us in the following to optically access the DE via the spin-blockaded biexciton state with ±3 spin projection.

Next, we study the properties of the DE state itself. The preparation of the DE is performed by detecting a photon due to recombination of the $XX^0_{\mathrm{T}\pm3}$ biexciton. This photon heralds the presence of the DE inside the QD. In addition, the circular polarization of this photon also determines the initial spin-state of the DE. Afterwards, the DE spin evolves in time. If a single photo-excited charge carrier (electron or hole) with a spin opposite to that of the DE is captured by the QD, then the DE is converted into an optically active trion. This trion radiatively recombines and the emitted circularly polarized photon "reads out" the spin state of the DE at the time of the charging event. Due to the continuous wetting-layer excitation chosen in our experiments, the formation of the $XX^0_{\mathrm{T}\pm3}$ state as well as the DE spin read out are both stochastic processes. The photo-generated charge carriers are randomly captured by the QD at a rate, which is proportional to the intensity of the exciting light. By tuning the excitation energy, intensity, and sample temperature, the average charge state of the QD and the charge-carrier capture rate can be controlled to some extent.[33] This has been used in our experiment to adjust the detection rates for photons from the $XX^0_{\mathrm{T}\pm3}$ state and the respective trion state.

Figure 3(a) presents the measured normalized cross-correlation events between the $XX^0_{\mathrm{T}\pm3}$ state and the X^+ trion state for co- and cross-circular polarizations. Here, SSPDs were employed for

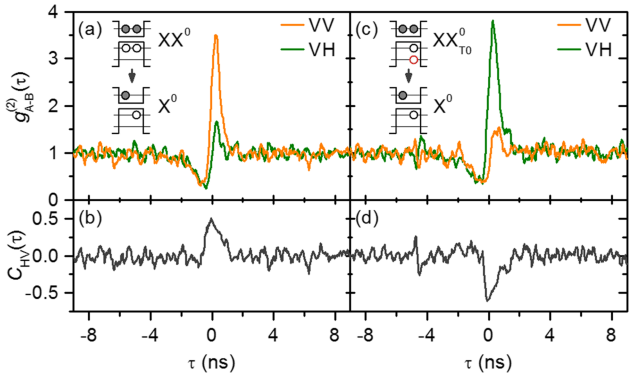

FIG. 2. Polarization sensitive measurements of the photon cross-correlation $g^{(2)}_{\mathrm{A\text{-}B}}(\tau)$ and extracted degree of rectilinear (HV) polarization correlation $C_{\mathrm{HV}}(\tau)$ for the two different radiative cascades: [(a) and (b)] the spin-singlet biexciton-exciton (XX^0-X^0) cascade and [(c) and (d)] the spin-triplet biexciton-exciton (XX^0_{T0}-X^0) cascade. Schematics show the charge-carrier configuration of the QD initial states leading to the respective photon detection. Strong bunching is observed in both cases confirming the biexcitonic origin of the initial states. For the XX^0_{T0}-X^0 cascade, bunching is observed in cross-rectilinear polarization measurements (VH), in contrast to the XX^0-X^0 cascade, confirming the selection rules and energy level alignment illustrated in Fig. 1(c).

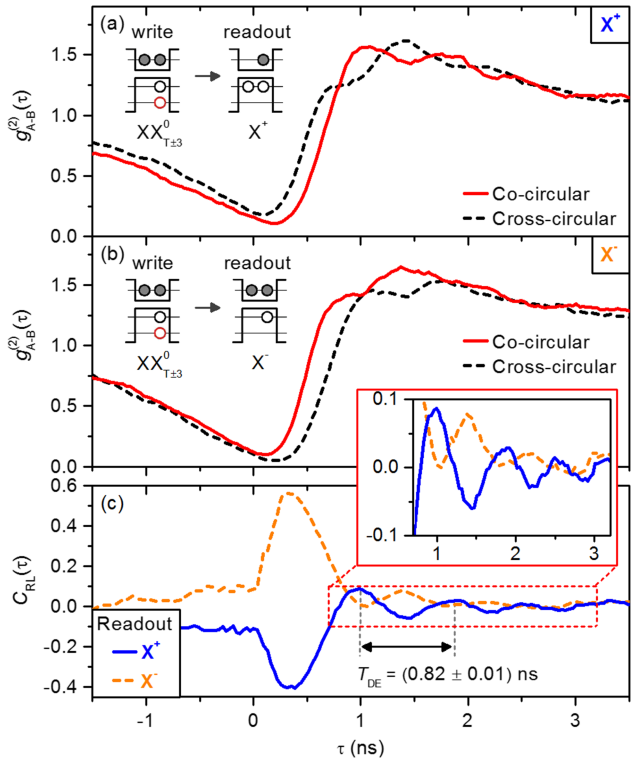

FIG. 3. Photon cross-correlation experiments between the $XX^0_{T\pm3}$ state (dark exciton (DE) preparation) and the charged trion states (DE read-out). (a) X^+ and (b) X^- (cf. schematics for the respective charge-carrier configuration). The solid and dashed lines correspond to co- (LL + RR) and cross- (RL + LR) circular polarization, respectively. (c) Degree of correlation in circular polarization $C_{RL}(\tau)$ extracted from the measurement data presented in (a) and (b). Due to the precession of the dark exciton (DE) spin between preparation and readout, oscillations occur with a period T_{DE} revealing a DE fine-structure splitting of (5.0 ± 0.7) μeV.

improved timing resolution (cf. setup description). The experimental conditions, i.e., P = 2.0 μW, λ = 877.2 nm, and T = 17.7 K, were carefully chosen to achieve comparable detection rates from both spectral lines while simultaneously providing low population of the bright exciton. We observe a pronounced photon bunching at positive delay times, resulting from the QD charging, which converts the DE into the bright trion X^+. The correlated signal at positive times exhibits oscillations with opposite phase for co- and cross-circular polarizations. These oscillations result from the coherent precession of the DE's spin as reported in Ref. 16. Due to a finite fine-structure splitting $\Delta E_{FSS,DE}$ between the DE eigenstates $|\uparrow\Uparrow \pm \downarrow\Downarrow\rangle$,[34] a coherent superposition of these states, heralded by the detection of a circularly polarized $XX^0_{T\pm3}$ photon, precesses in time with a period of $T_{DE} = h/E_{FSS,DE}$, where h is Planck's constant. Similar observation is obtained for the case in which the readout of the DE is performed via the negatively charged trion X^-, as presented in Fig. 3(b) (P = 1.8 μW, λ = 877.2 nm and T = 9.5 K). The phase of the oscillations for co- and cross-circular polarization correlations, however, is reversed compared to the readout via the X^+ state. This becomes more evident in Fig. 3(c), where the degree of circular correlation $C_{RL}(\tau)$ deduced from the experimental data shown in (a) and (b) is displayed. Here we are able to observe up to 4 complete spin-precession cycles of the DE state. The relatively strong damping of the oscillations is mainly due to the applied CW non-resonant excitation scheme.[16] This masks the intrinsic coherence time of the DE, which was measured to be about 100 ns using pulsed-resonant excitation.[20] Fitting the experimental data in Fig. 3(c) with an exponentially damped cosine function reveals a precession period of the DE of T_{DE} = (0.82 ± 0.01) ns, corresponding to a fine-structure splitting of $\Delta E_{FSS,BE}$ = (5.0 ± 0.7) μeV. The fast precession of the DE in our QD microlens would in principle allow for an about 4-times faster rate of entangled-photon generation compared to that reported in Ref. 21, where the DE has been used as an entangler with $T_{DE} \approx 3$ ns.

In summary, we demonstrated the all-optical preparation and readout of the DE spin using deterministic microlenses defined above pre-selected QDs. By clearly observing the coherent spin precession in deterministically processed devices grown via MOCVD, we provide evidence for the robustness of the DE as a long-lived coherent spin qubit and pave the way for wider applications. Our work thus constitutes an important step toward scalable implementations of quantum information schemes exploiting the DE spin-qubit, such as photonic cluster state generation.[21] Employing further technological improvements, such as a backside gold mirror[35] and integrated micro-objectives,[36] we expect to achieve photon extraction efficiencies of up to 80% in future experiments. Exploiting the DE spin-qubit in deterministic devices supplied with electrical contacts[37] could lead to significantly improved entanglement fidelities compared to protocols based on all-optical pulse sequences.[38]

Expert sample preparation by R. Schmidt and technical support by C. Hopfmann are gratefully acknowledged. This project has received funding from the German Research Foundation (DFG) within the Collaborative Research Center CRC 787 "Semiconductor Nanophotonics: Materials, Models, Devices", the German-Israeli-Foundation for Scientific Research and Development (GIF), Grant No. 1148-77.14/2011, and the European Research Council (ERC) under the European Union's Horizon 2020 research and innovation program (grant agreement No 695188). T.H. acknowledges support by the COST Action MP1403 "Nanoscale Quantum Optics" via a STSM-Grant. Furthermore, we acknowledge support by the DFG and the Open Access Publication Funds of Technische Universität Berlin.

[1] T. D. Ladd, F. Jelezko, R. Laflamme, Y. Nakamura, C. Monroe, and J. L. O'Brien, Nature **464**, 45 (2010).
[2] A. Imamoglu, D. D. Awschalom, G. Burkard, D. P. DiVincenzo, D. Loss, M. Sherwin, and A. Small, Phys. Rev. Lett. **83**, 4204 (1999).
[3] I. Aharonovich, D. Englund, and M. Toth, Nat. Photonics **10**, 631 (2016).
[4] A. Schlehahn, A. Thoma, P. Munnelly, M. Kamp, S. Höfling, T. Heindel, C. Schneider, and S. Reitzenstein, APL Photonics **1**, 011301 (2016).
[5] T. Heindel, A. Thoma, M. von Helversen, M. Schmidt, A. Schlehahn, M. Gschrey, P. Schnauber, J. H. Schulze, A. Strittmatter, J. Beyer, S. Rodt, A. Carmele, A. Knorr, and S. Reitzenstein, Nat. Commun. **8**, 14870 (2017).
[6] A. Orieux, M. A. M. Versteegh, K. D. Jöns, and S. Ducci, Rep. Prog. Phys. **80**, 076001 (2017).
[7] N. H. Bonadeo, E. J. Erland, D. Gammon, D. Park, D. S. Katzer, and D. G. Steel, Science **282**, 1473 (1998).
[8] A. Zrenner, E. Beham, S. Stufler, F. Findeis, M. Bichler, and G. Abstreiter, Nature **418**, 612 (2002).
[9] D. Press, T. D. Ladd, B. Zhang, and Y. Yamamoto, Nature **456**, 218 (2008).
[10] K. De Greve, P. L. McMahon, D. Press, T. D. Ladd, D. Bisping, C. Schneider, M. Kamp, L. Worschech, S. Höfling, A. Forchel, and Y. Yamamoto, Nat. Phys. **7**, 872 (2011).
[11] P. Michler, *Quantum Dots for Quantum Information Technologies* (Springer International Publishing, 2017).
[12] E. Poem, O. Kenneth, Y. Kodriano, Y. Benny, S. Khatsevich, J. E. Avron, and D. Gershoni, Phys. Rev. Lett. **107**, 087401 (2011).
[13] Y. Benny, S. Khatsevich, Y. Kodriano, E. Poem, R. Presman, D. Galushko, P. M. Petroff, and D. Gershoni, Phys. Rev. Lett. **106**, 040504 (2011).
[14] Y. Kodriano, I. Schwartz, E. Poem, Y. Benny, R. Presman, T. A. Truong, P. M. Petroff, and D. Gershoni, Phys. Rev. B **85**, 241304(R) (2012).
[15] J. McFarlane, P. A. Dalgarno, B. D. Gerardot, R. H. Hadfield, R. J. Warburton, K. Karrai, A. Badolato, and P. M. Petroff, Appl. Phys. Lett. **94**, 093113 (2009).
[16] E. Poem, Y. Kodriano, C. Tradonsky, N. H. Lindner, B. D. Gerardot, P. M. Petroff, and D. Gershoni, Nat. Phys. **6**, 993 (2010).
[17] S. Lüker, T. Kuhn, and D. E. Reiter, Phys. Rev. B **92**, 201305 (2015).
[18] L. Gantz, E. R. Schmidgall, I. Schwartz, Y. Don, E. Waks, G. Bahir, and D. Gershoni, Phys. Rev. B **94**, 045426 (2016).
[19] I. Schwartz, D. Cogan, E. R. Schmidgall, L. Gantz, Y. Don, M. Zieliński, and D. Gershoni, Phys. Rev. B **92**, 201201(R) (2015).
[20] I. Schwartz, E. R. Schmidgall, L. Gantz, D. Cogan, E. Bordo, Y. Don, M. Zieliński, and D. Gershoni, Phys. Rev. X **5**, 011009 (2015).
[21] I. Schwartz, D. Cogan, E. R. Schmidgall, Y. Don, L. Gantz, O. Kenneth, N. H. Lindner, and D. Gershoni, Science **354**, 434 (2016).
[22] Y. Kodriano, E. Poem, N. H. Lindner, C. Tradonsky, B. D. Gerardot, P. M. Petroff, J. E. Avron, and D. Gershoni, Phys. Rev. B **82**, 155329 (2010).
[23] G. Hönig, G. Callsen, A. Schliwa, S. Kalinowski, C. Kindel, S. Kako, Y. Arakawa, D. Bimberg, and A. Hoffmann, Nat. Commun. **5**, 5721 (2014).
[24] E. R. Schmidgall, I. Schwartz, D. Cogan, L. Gantz, and D. Gershoni, "Coherent control of dark excitons in semiconductor quantum dots," in *Quantum Dots for Quantum Information Technologies*, edited by P. Michler (Springer International Publishing, 2017), pp. 123–164.
[25] M. Gschrey, A. Thoma, P. Schnauber, M. Seifried, R. Schmidt, B. Wohlfeil, L. Krüger, J.-H. Schulze, T. Heindel, S. Burger, F. Schmidt, A. Strittmatter, S. Rodt, and S. Reitzenstein, Nat. Commun. **6**, 7662 (2015).

[26] M. Gschrey, F. Gericke, A. Schüssler, R. Schmidt, J.-H. Schulze, T. Heindel, S. Rodt, A. Strittmatter, and S. Reitzenstein, Appl. Phys. Lett. **102**, 251113 (2013).
[27] T. Heindel, S. Rodt, and S. Reitzenstein, "Single-photon sources based on deterministic quantum-dot microlenses," in *Quantum Dots for Quantum Information Technologies*, edited by P. Michler (Springer International Publishing, 2017), pp. 199–232.
[28] A. Schlehahn, M. Gaafar, M. Vaupel, M. Gschrey, P. Schnauber, J.-H. Schulze, S. Rodt, A. Strittmatter, W. Stolz, A. Rahimi-Iman, T. Heindel, M. Koch, and S. Reitzenstein, Appl. Phys. Lett. **107**, 041105 (2015).
[29] A. Thoma, P. Schnauber, M. Gschrey, M. Seifried, J. Wolters, J.-H. Schulze, A. Strittmatter, S. Rodt, A. Carmele, A. Knorr, T. Heindel, and S. Reitzenstein, Phys. Rev. Lett. **116**, 033601 (2016).
[30] T. Jakubczyk, V. Delmonte, S. Fischbach, D. Wigger, D. E. Reiter, Q. Mermillod, P. Schnauber, A. Kaganskiy, J.-H. Schulze, A. Strittmatter, S. Rodt, W. Langbein, T. Kuhn, S. Reitzenstein, and J. Kasprzak, ACS Photonics **3**, 2461–2466 (2016).
[31] E. Moreau, I. Robert, L. Manin, V. Thierry-Mieg, J. M. Gérard, and I. Abram, Phys. Rev. Lett. **87**, 183601 (2001).
[32] Y. Kodriano, E. R. Schmidgall, Y. Benny, and D. Gershoni, Semicond. Sci. Technol. **29**, 053001 (2014).
[33] Y. Benny, Y. Kodriano, E. Poem, D. Gershoni, T. A. Truong, and P. M. Petroff, Phys. Rev. B **86**, 085306 (2012).
[34] M. Bayer, G. Ortner, O. Stern, A. Kuther, A. A. Gorbunov, A. Forchel, P. Hawrylak, S. Fafard, K. Hinzer, T. L. Reinecke, S. N. Walck, J. P. Reithmaier, F. Klopf, and F. Schäfer, Phys. Rev. B **65**, 195315 (2002).
[35] S. Fischbach, A. Kaganskiy, E. B. Y. Tauscher, F. Gericke, A. Thoma, R. Schmidt, A. Strittmatter, T. Heindel, S. Rodt, and S. Reitzenstein, Appl. Phys. Lett. **111**, 011106 (2017).
[36] S. Fischbach, A. Schlehahn, A. Thoma, N. Srocka, T. Gissibl, S. Ristok, S. Thiele, A. Kaganskiy, A. Strittmatter, T. Heindel, S. Rodt, A. Herkommer, H. Giessen, and S. Reitzenstein, ACS Photonics **4**, 1327 (2017).
[37] A. Schlehahn, R. Schmidt, C. Hopfmann, J.-H. Schulze, A. Strittmatter, T. Heindel, L. Gantz, E. R. Schmidgall, D. Gershoni, and S. Reitzenstein, Appl. Phys. Lett. **108**, 021104 (2016).
[38] E. R. Schmidgall, I. Schwartz, D. Cogan, L. Gantz, T. Heindel, S. Reitzenstein, and D. Gershoni, Appl. Phys. Lett. **106**, 193101 (2015).